Inorg. Chem. **1991**, *30*, 2062-2066

Contribution from the Department of Chemistry, University of Ottawa, Ottawa, Ontario K1N 6N5, Canada,
Laboratorium voor Anorganische Chemie, Rijksuniversiteit Groningen, Nijenborgh 16, 9747 AG Groningen, The Netherlands,
and Vakgroep Algemene Chemie, Afdeling Kristal-en Structuurchemie, Rijksuniversiteit Utrecht,
Padualaan 8, 3584 CH Utrecht, The Netherlands

Synthesis and Structural Features of Novel Vanadium(II) Amides. X-ray Structures of Octahedral $[(2\text{-}C_5H_4N)(CH_3)N]_2V(TMEDA)$ (TMEDA = *N,N,N′,N′*-Tetramethylethylenediamine) and Square-Pyramidal $[2,5\text{-}(CH_3)_2C_4H_2N]_2V(Py)_3$ (Py = Pyridine)

Jilles J. H. Edema,[†] Sandro Gambarotta,*[,†] Auke Meetsma,[‡] Anthony L. Spek,[§] and Nora Veldman[§]

Received September 4, 1990

The reaction of *trans*-$(TMEDA)_2VCl_2$ (TMEDA = *N,N,N′,N′*-tetramethylethylenediamine) with both mono- and bidentate alkali-metal amides has been investigated. Utilization of 2 equiv of bidentate amide (N⌒N)–M [M = Li, Na; N⌒N = 2-$(MeN)C_5H_4N$ (**1**), PhNNNPh (**2**), 7-azaindolyl (**3**), PhNCHCNPh (**4**), $(C_5H_4N)_2N$ (**5**)] led to the formation of the corresponding monomeric and octahedral $(R_2N)_2V(TMEDA)$ species. A spontaneous dimerization reaction was obtained in the case of the acetanilide PhNC(Me)O ligand, allowing the isolation of the nearly diamagnetic dimer $[PhNC(Me)O]_4V_2(TMEDA)$ (**6**). While the compounds obtained with monodentate amide showed a high tendency to disproportionate, an unusual square-pyramidal monomeric complex $[2,5\text{-}(CH_3)_2C_4H_2N]_2V(Py)_3$ (Py = pyridine) (**9**) was formed, in the case of the pyrrolyl derivative, under the usual reaction conditions, followed by in situ treatment of the reaction mixture with pyridine. Crystal data for **1** and **9** are as follows. **1** [$T = 100$ K, λ(Mo Kα) = 0.71073 Å]: monoclinic, space group $P2_1/n$, $a = 10.075$ (1) Å, $b = 13.731$ (2) Å, $c = 15.102$ (2) Å, $\beta = 108.50$ (1)°, $V = 1981.2$ (5) Å^3, $Z = 4$, $d_{calcd} = 1.279$ g cm^{-3}, $\mu = 5.0$ cm^{-1}, $F(000) = 812$, $R = 0.047$ ($R_w = 0.066$). **9** [$T = 298$ K, λ(Mo Kα) = 0.71073 Å]: monoclinic, space group $P2_1/n$, $a = 11.072$ (3) Å, $b = 13.067$ (1) Å, $c = 17.251$ (5) Å, $\beta = 92.85$ (1)°, $V = 2532$ (1) Å^3, $Z = 4$, $d_{calcd} = 1.250$ g cm^{-3}, $\mu = 4.0$ cm^{-1}, $F(000) = 1004$, $R = 0.047$ ($R_w = 0.026$).

Introduction

In the recent literature, there has been a steady growth of interest in the synthesis, structural characterization, and reactivity of transition-metal complexes using organic amides as supporting ligands.[1] Among the features that make these ligands especially attractive is the strong basicity of the amide group, which is crucial for both the stabilization of a wide range of oxidation states (a versatile chemical reactivity having been recently shown for example in the case of trivalent tungsten and molybdenum,[2a,f] and tetravalent zirconium[2g]) and for favoring di- and polynuclear aggregation, through bridging interactions of the nitrogen donor atom with two or more metal centers.[3] This second possibility turns out to be especially attractive in the chemistry of low-valent vanadium, where bridging interactions may prelude the occurrence of short intermetallic contacts and, ultimately, the formation of metal–metal bonds.[4]

The lack of suitable V(II) starting materials has hampered the systematic development of the chemistry of divalent vanadium, limited so far to a quite large collection of diversified complexes.[5,6] While the structures and the chemical behavior of vanadium(II) acetate,[5m,n] alkoxide,[5i,j] and aryl[6d] complexes have been clarified only in the very recent literature, vanadium(II) amides remain largely unknown and limited to only one example.[5k] However, organic amides are expected to be especially versatile for the stabilization of the oxidation state (+II), due to the apparent great stability of the V–N bond,[6] hopefully able to prevent unwanted disproportionation reactions.[7]

We have now attempted the preparation of a novel class of vanadium(II) amides, using both mono- and bidentate organic amides. In this preliminary paper, we describe the straightforward synthesis and some unexpected structural features.

Experimental Section

All operations were performed under an inert atmosphere (N_2 or Ar), using standard Schlenk techniques, or in a nitrogen-filled drybox (Vacuum Atmospheres). *trans*-$(TMEDA)_2VCl_2$ was prepared according to published procedures.[6d] TMEDA (TMEDA = *N,N,N′,N′*-tetramethylethylenediamine), Cy_2NH, Et_2NH, and *i*-Pr_2NH were chromatographed over Al_2O_3 and distilled over molten potassium, after refluxing. 2-$(MeNH)C_5H_4N$, PhNNN(H)Ph, 7-azaindole, *N,N′*-diphenylformamide, $(C_5H_4N)_2NH$, phenylacetamide, Ph_2NH, carbazole, 3,5-dimethylpyrazole, and 2,5-$Me_2C_4H_2NH$ were used as received (Aldrich). Infrared

Table I. Crystal Data and Structural Analysis Results

	1	**9**
formula	$C_{18}H_{30}N_6V$	$C_{27}H_{31}N_5V$
M_r	381.42	476.52
cryst syst	monoclinic	monoclinic
space group	$P2_1/n$	$P2_1/n$
Z	4	4
a, Å	10.075 (1)	11.072 (3)
b, Å	13.731 (2)	13.067 (1)
c, Å	15.102 (2)	17.521 (2)
β, deg	108.50 (1)	92.85 (2)
V, Å^3	1981.2 (5)	2532 (1)
d_{calcd}, g cm^{-3}	1.279	1.250
$F(000)$	812	1004
μ_{calcd}, cm^{-1}	5.0	4.0
λ(Mo Kα), Å	0.71073	0.71073
T, K	100	295
θ range, deg: max, min	1.42, 24.19	1.17, 28.0
no. of tot. data	3319	6530
no. of unique data	3030	6080
no. of obsd data	2242 [$I \geq 2.5\sigma(I)$]	3465 [$I \geq 2.5\sigma(I)$]
no. of params	250	393
R, R_w, S	0.047, 0.066, 1.35	0.047, 0.026, 2.037

[†] University of Ottawa.
[‡] Rijksuniversiteit Groningen.
[§] Rijksuniversiteit Utrecht.

(1) (a) Lappert, M. F.; Power, P. P.; Sanger, A. R.; Srivastava, R. C. *Metal and Metalloid Amides*; Ellis Norwood Ltd.: Chichester, England, 1980; see also references cited therein. (b) Hope, H.; Olmstead, M. M.; Murray, B. D.; Power, P. P. *J. Am. Chem. Soc.* **1985**, *107*, 712. (c) Murray, B. D.; Power, P. P. *Inorg. Chem.* **1984**, *23*, 4584. (d) Chen, H.; Bartlet, R. A.; Olmstead, M. M.; Power, P. P.; Shoner, S. C. *J. Am. Chem. Soc.* **1990**, *112*, 1048 and references cited therein. (e) Andersen, R. A.; Faegri, K.; Green, J. C.; Haaland, A.; Lappert, M. F.; Leung, W. P.; Rypdal, K. *Inorg. Chem.* **1988**, *27*, 1782. (f) Bradley, D. C.; Hursthouse, M. B.; Malik, K. M. A.; Moseler, R. *Transition Met. Chem.* (*London*) **1978**, *3*, 253.

(2) (a) Blatchford, T. P.; Chisholm, M. H.; Huffman, J. C. *Inorg. Chem.* **1987**, *26*, 1920. (b) Chisholm, M. H.; Cotton, F. A.; Frenz, B. A.; Reichert, W. W.; Shive, L. W.; Stilts, B. R. *J. Am. Chem. Soc.* **1976**, *98*, 4469. (c) Chisholm, M. H.; Huffman, J. C.; Smith, C. A. *J. Am. Chem. Soc.* **1986**, *108*, 222. (d) Ahmed, K. J.; Chisholm, M. H.; Folting, K.; Huffman, J. C. *J. Am. Chem. Soc.* **1986**, *108*, 989. (e) Chisholm, M. H.; Hammond, C. E.; Ho, D.; Huffman, J. C. *J. Am. Chem. Soc.* **1986**, *108*, 7860. (f) Chisholm, M. H.; Hammond, C. E.; Huffman, J. C. *J. Chem. Soc., Chem. Commun.* **1987**, 1423. (g) Cummins, C. C.; Baxter, S. M.; Wolczanski, P. T. *J. Am. Chem. Soc.* **1988**, *110*, 8731.

0020-1669/91/1330-2062$02.50/0

spectra were recorded on a Perkin-Elmer 393 instrument from Nujol mulls prepared in a drybox. Elemental analyses were carried out at the Microanalytical Department of the Chemistry Department at the Rijksuniversiteit Groningen. Samples for magnetic susceptibility measurements were weighed inside a drybox equipped with a microanalytical balance and sealed into a specially designed Teflon capsule. Data were recorded at variable temperatures in the range 100–298 K by using a Faraday balance (Oxford Instruments) interfaced with an Apple II computer. Plots of $1/\chi_g$ against T (K) were in satisfactory agreement with the Curie–Weiss law in all cases. Magnetic moments were calculated by following standard methods,[8a] and corrections for underlying diamagnetism were applied to the data.[8b]

[(2-C_5H_4N)(CH_3)N]$_2$V(TMEDA) (1). A solution of *n*-BuLi in hexane (5.3 mL, 2.5 N, 13.2 mmol) was added to a cooled solution (−80 °C) of (2-C_5H_4N)(CH_3)NH (1.45 g, 13.2 mmol) in THF (40 mL). The mixture was stirred for 30 min and gradually warmed to room temperature. The addition of solid $VCl_2(TMEDA)_2$ (2.26 g, 6.4 mmol) turned the color to deep red. After 12 h of stirring, the solvent was removed in vacuo and the residual solid recrystallized at −30 °C from Et_2O (50 mL), yielding dark red air-sensitive crystals of **1** (1.86 g, 4.9 mmol, yield 76%). Anal. Calcd (found) for $C_{18}H_{30}N_6V$: C, 56.68 (56.37); H, 7.93 (7.85); N, 22.03 (21.68); V, 13.36 (13.41). IR (Nujol mull, KBr, cm^{-1}): 1585 (s), 1560 (w), 1530 (m), 1480 (s), 1400 (s), 1300 (s), 1260 (m), 1145 (s), 1120 (w), 1115 (w), 1095 (w), 1070 (m), 1030 (s), 1005 (m), 985 (s), 965 (m), 820 (m), 795 (s), 750 (s), 725 (s), 630 (m), 595 (m), 530 (m), 485 (m). ($\mu_{eff} = 3.68\ \mu_B$.)

(PhN=NNPh)$_2$V(TMEDA) (2). A solution of *n*-BuLi in hexane (3.0 mL, 2.5 N, 7.5 mmol) was added to a cooled solution (−80 °C) of diphenyltriazine in THF (40 mL). The mixture was gradually warmed to room temperature, and solid $VCl_2(TMEDA)_2$ (1.27 g, 3.6 mmol) was added. The resulting mixture was stirred at room temperature for 12 h. After solvent evaporation in vacuo, the residual solid was crystallized from Et_2O (25 mL) at −80 °C, yielding deep red air-sensitive crystals of **2** (1.46 g, 2.6 mmol, yield 73%). Anal. Calcd (found) for $C_{30}H_{36}N_8V$: C, 64.39 (64.23); H, 6.48 (6.28); N, 20.02 (19.86); V, 9.10 (9.27). IR (Nujol mull, KBr, cm^{-1}): 1590 (s), 1420 (s), 1375 (m), 1340 (m), 1320 (m), 1290 (m), 1270 (s), 1220 (m), 1160 (s), 1120 (w), 1070 (m), 1050 (w), 1015 (m), 995 (m), 950 (s), 820 (w), 800 (s), 775 (s), 770 (s), 690 (s), 665 (s), 605 (s), 520 (w), 500 (m). ($\mu_{eff} = 3.81\ \mu_B$.)

(7-azaindolyl)$_2$V(TMEDA) (3). A solution of 7-azaindole (1.82 g, 15.4 mmol) in THF (100 mL) was stirred with NaH (0.38 g, 15.8 mmol) for 30 min. Addition of solid $VCl_2(TMEDA)_2$ (2.67 g, 7.5 mmol) to the mixture resulted in an orange-red suspension. After the mixture was filtered and evaporated to dryness, the residual solid was resuspended in Et_2O (50 mL). THF was added dropwise until the solid dissolved. Orange air-sensitive crystals of **3** (1.93 g, 4.8 mmol, yield 64%) were obtained upon cooling the resulting solution at −30 °C. Anal. Calcd (found) for $C_{20}H_{26}N_6V$: C, 59.84 (59.87); H, 6.53 (6.48); N, 20.94 (20.93); V, 12.69 (12.62). IR (Nujol mull, KBr, cm^{-1}): 1575 (s), 1550 (w), 1410 (m), 1400 (w), 1360 (s), 1350 (w), 1320 (s), 1300 (s), 1280 (w), 1255 (w), 1200 (m), 1160 (s), 1115 (m), 1055 (m), 1015 (w), 1000 (w), 945 (s), 915 (s), 905 (s), 800 (s), 770 (s), 730 (m), 715 (s), 665 (w). ($\mu_{eff} = 3.73\ \mu_B$.)

[PhN=C(H)NPh]$_2$V(TMEDA) (4). NaH (0.34 g, 14.2 mmol) was suspended in a solution of diphenylformamidine, PhN(H)CH=NPh (2.77 g, 14.1 mmol) in THF (75 mL). After the mixture was stirred for 15 min, *trans*-$VCl_2(TMEDA)_2$ (2.4 g, 6.9 mmol) was added and stirring was continued for 10 h. The color of the mixture gradually turned reddish brown, and a white solid (NaCl) separated. After filtration and solvent evaporation in vacuo, the residual solid was recrystallized from Et_2O (50 mL) at −30 °C, yielding brick red air-sensitive crystals of **4** (2.98 g, 4.7 mmol, 68%). Anal. Calcd (found) for $C_{32}H_{38}N_6V$: C, 68.92 (68.70); H, 6.87 (6.75); N, 15.07 (15.04); V, 9.14 (8.90). IR (Nujol mull, KBr, cm^{-1}): 1670 (m), 1585 (m), 1470 (s), 1390 (m), 1465 (m), 1365 (m), 1275 (s), 1265 (s), 1210 (s), 1165 (m), 1055 (s), 1010 (m), 990 (w), 955 (m), 930 (w), 820 (w), 795 (s), 775 (s), 755 (s), 690 (s), 660 (w). ($\mu_{eff} = 3.76\ \mu_B$).

[(C_5H_4N)$_2$N]$_2$V(TMEDA) (5). A solution of $(C_5H_4N)_2NH$ (1.17 g, 6.84 mmol) in THF (75 mL) was stirred with NaH (0.16 g, 6.8 mmol) for 20 min. Addition of solid $VCl_2(TMEDA)_2$ (1.18 g, 3.3 mmol) resulted in the formation of a red-purple color. After 5 h of stirring, the mixture was filtered and the volume was reduced to approximately 50 mL. Deep red air-sensitive needles of **5** (1.24 g, 2.4 mmol, 73% yield) separated upon cooling at −30 °C. Anal. Calcd (found) for $C_{26}H_{32}N_8V$: C, 61.53 (61.65); H, 6.36 (6.40); N, 22.08 (21.93); V, 10.04 (9.97). IR (Nujol mull, KBr, cm^{-1}): 1585 (s), 1570 (s), 1530 (m), 1470 (s), 1430 (s), 1370 (s), 1310 (m), 1280 (w), 1250 (m), 1150 (w), 1140 (s), 1095 (w), 1050 (m), 1010 (s), 920 (s), 840 (m), 750 (s), 720 (s), 530 (m), 490 (w). ($\mu_{eff} = 3.83\ \mu_B$.)

{[PhNC(Me)O]$_2$V}$_2$(TMEDA) (6). NaH (0.28 g, 11.6 mmol) was suspended in a solution of PhNHC(O)Me (1.5 g, 11.5 mmol) in THF (50 mL). The resulting mixture was stirred for 30 min. A red color formed upon addition of *trans*-$(TMEDA)_2VCl_2$ (1.83 g, 5.17 mmol), and stirring was continued for an additional 8 h. After solvent evaporation in vacuo, the resulting red solid was recrystallized from Et_2O (25 mL) at −30 °C, yielding large red air-sensitive crystals of **3** (1.31 g, 1.7 mmol, 67%). Anal. Calcd (found) for $C_{38}H_{48}N_6O_4V_2$: C, 60.47 (59.96); H, 6.41 (6.21); N, 11.14 (10.95); V, 13.50 (13.29). IR (Nujol mull, KBr, cm^{-1}): 1550 (s), 1400 (s), 1350 (s), 1280 (m), 1235 (s), 1225 (s), 1170 (w), 1160 (w), 1150 (w), 1120 (w), 1065 (m), 1025 (s), 1010 (s), 955 (s), 925 (w), 895 (m), 820 (m), 810 (m), 790 (s), 750 (s), 695 (s), 665 (w), 655 (m). ($\mu_{eff} = 0.42\ \mu_B$.)

[(Cy_2N)$_2$V]$_2$ (7). An ether solution of MeLi (9.7 mL, 1.4 M, 13.6 mmol) was added to a cooled (−80 °C) solution of Cy_2NH (2.75 mL, 13.6 mmol) in THF (80 mL). The mixture was warmed to room temperature and then cooled to −40 °C. The addition of $VCl_2(TMEDA)_2$ (2.36 g, 6.7 mmol) resulted in a deep red color. After being stirred for 3 h, the mixture was warmed to room temperature. The solvent was evaporated in vacuo and the residual solid recrystallized from hexane (50 mL), yielding red-brown air-sensitive crystals of **7** (1.15 g, 1.40 mmol, yield 42%). Anal. Calcd (found) for $C_{24}H_{44}N_2V$: C, 70.04 (69.48); H, 10.78 (10.90); N, 6.81 (6.75); V, 12.38 (12.38). IR (Nujol mull, KBr, cm^{-1}): 1440 (s), 1350 (s), 1330 (m), 1240 (s), 1160 (m), 1140 (s), 1110 (s), 1090 (s), 1025 (s), 970 (w), 940 (s), 880 (m), 830 (m), 800 (w), 770 (w), 700 (w), 680 (m), 580 (m), 510 (w), 490 (s), 450 (w), 420 (w). ($\mu_{eff} = 2.28\ \mu_B$.)

[2,5-Me_2(C_4H_2N)]$_2$V(Py)$_3$ (9). Neat 2,5-$(CH_3)_2C_4H_2NH$ (1.35 mL, 13.3 mmol) was added to a suspension of NaH (0.32 g, 13.4 mmol) in THF (50 mL). The mixture was stirred and refluxed for 30 min and treated with *trans*-$(TMEDA)_2VCl_2$ (2.42 g, 13.3 mmol). A red color gradually appeared, and stirring was continued for 14 h. The red solution was filtered and treated with pyridine (5 mL). Red air-sensitive crystals of **9** were formed upon standing at room temperature (2.67 g, 5.61 mmol, yield 82%). Anal. Calcd (found) for $C_{27}H_{31}N_5V$: C, 68.05 (67.73); H, 6.56 (6.38); N, 14.70 (14.49); V, 10.69 (10.68). IR (Nujol mull, KBr,

---

(3) (a) Sheldrick, W. S. *J. Fluorine Chem.* **1974**, *4*, 415. (b) Chisholm, M. H.; Cotton, F. A.; Extine, M. W.; Rideout, C. D. *Inorg. Chem.* **1978**, *17*, 3536. (c) Bradley, D. C. *Adv. Inorg. Chem. Radiochem.* **1972**, *15*, 259. (d) Eller, P. G.; Bradley, D. C.; Hursthouse, M. B.; Meek, D. W. *Coord. Chem. Rev.* **1977**, *24*, 1. (e) Rogers, R. D.; Atwood, J. L.; Gruning, R. *J. Organomet. Chem.* **1978**, *157*, 229. (f) Bradley, D. C.; Hursthouse, M. B.; Malik, K. M. A.; Moseler, R. *Transition Met. Chem.* (*London*) **1978**, 3253. (g) Barr, D.; Clegg, W.; Mulvey, R. E.; Snaith, R. *J. Chem. Soc., Chem. Commun.* **1984**, 285. (h) Edema, J. J. H.; Gambarotta, S.; Spek, A. L. *Inorg. Chem.* **1989**, *28*, 811.

(4) (a) Seidel, W.; Kreisel, G.; Mennenga, H. *Z. Chem.* **1976**, *16*, 492. (b) Cotton, F. A.; Millar, M. *J. Am. Chem. Soc.* **1977**, *99*, 7886. (c) Cotton, F. A.; Lewis, G. E.; Mott, G. N. *Inorg. Chem.* **1983**, *22*, 560. (d) Cotton, F. A.; Diebold, M. P.; Shim, I. *Inorg. Chem.* **1985**, *24*, 1510.

(5) (a) Vilas Boas, L.; Costa Pessoa, J. In *Comprehensive Coordination Chemistry*; Wilkinson, G., Ed.; Pergamon Press: Oxford, England, 1987; Vol. 3. (b) Girolami, G. S.; Wilkinson, G.; Galas, A. M. R.; Thornton-Pett, M.; Hursthouse, M. B. *J. Chem. Soc., Dalton Trans.* **1985**, 1339. (c) Jensen, J. A.; Girolami, G. S. *Inorg. Chem.* **1989**, *28*, 2114. (d) Cotton, F. A.; Duraj, S. A.; Roth, W. J. *Inorg. Chem.* **1985**, *24*, 913. (e) Oumous, H.; Lecompte, C.; Protas, J.; Poncet, J. L.; Barbe, J. M.; Guilard, R. *J. Chem. Soc., Dalton Trans.* **1984**, 2677. (f) Cotton, F. A.; Falvello, L. R.; Llusar, R.; Libby, E.; Murillo, C. A.; Schwotzer, W. *Inorg. Chem.* **1986**, *25*, 3423. (g) Olmstead, M. M.; Power, P. P.; Shoner, S. C. *Organometallics* **1988**, *7*, 1380. (h) Smith, P. D.; Martin, J. L.; Huffman, J. C.; Bansemer, R. L.; Caulton, K. G. *Inorg. Chem.* **1985**, *24*, 2997 and references cited therein. (i) Wilisch, W. C. A.; Armstrong, W. H.; Scott, W. J. *J. Am. Chem. Soc.* **1990**, *112*, 2429. (j) Floriani, C.; Mazzanti, M.; Chiesi-Villa, A.; Guastini, C. *Angew. Chem., Int. Ed. Engl.* **1988**, *27*, 576. (k) Cotton, F. A.; Poli, R. *Inorg. Chim. Acta* **1988**, *141*, 91. (l) Cotton, F. A.; Falvello, L. R.; Llusar, R.; Libby, E.; Murillo, C. A.; Schwotzer, W. *Inorg. Chem.* **1986**, *25*, 3423. (m) Cotton, F. A.; Extine, M. W.; Falvello, L. R.; Lewis, D. B.; Lewis, G. E.; Murillo, C. A.; Schwotzer, W.; Tomas, M.; Troup, J. M. *Inorg. Chem.* **1986**, *25*, 3505. (n) Gelmini, L.; Armstrong, W. H. *J. Chem. Soc., Chem. Commun.* **1989**, 1904.

(6) (a) Brauer, D. J.; Krüger, C. *Cryst. Struct. Commun.* **1973**, *3*, 421. (b) Dapporto, P.; Mani, F.; Mealli, C. *Inorg. Chem.* **1978**, *17*, 1323 and references cited therein. (c) Edema, J. J. H.; Meetsma, A.; Gambarotta, S. *J. Am. Chem. Soc.* **1989**, *111*, 6878. (d) Edema, J. J. H.; Stauthamer, W.; Gambarotta, S.; van Bolhuis, F.; Smeets, W. J. J.; Spek, A. L. *Inorg. Chem.* **1990**, *29*, 1302.

(7) Gambarotta, S.; van Bolhuis, F.; Chiang, M. Y. *Inorg. Chem.* **1987**, *26*, 4301.

(8) (a) Mabbs, M. B.; Machin, D. J. *Magnetism and Transition Metal Complexes*; Chapman and Hall: London, 1973. (b) Foese, G.; Gorter, C. J.; Smits, L. J. *Constantes Selectionnées Diamagnetisme, Paramagnetisme, Relaxation Paramagnetique*; Masson: Paris, 1957.

Table II. Fractional Atomic Coordinates and Equivalent Isotropic Thermal Parameters for **1**

atom	x	y	z	U_{eq}, Å^2
V	0.23865 (7)	0.20106 (6)	0.38869 (5)	0.0239 (2)
N1	0.4280 (4)	0.2836 (3)	0.4180 (2)	0.030 (1)
N2	0.4313 (3)	0.1220 (3)	0.4054 (2)	0.027 (1)
N3	0.1144 (4)	0.3174 (3)	0.4176 (3)	0.034 (1)
N4	0.2202 (3)	0.2076 (3)	0.5266 (2)	0.027 (1)
N5	0.1946 (4)	0.2056 (3)	0.2330 (2)	0.035 (1)
N6	0.0703 (3)	0.0874 (3)	0.3470 (3)	0.033 (1)
C1	0.5075 (4)	0.2020 (4)	0.4182 (3)	0.027 (1)
C2	0.6523 (5)	0.2134 (4)	0.4284 (3)	0.035 (2)
C3	0.7083 (5)	0.3048 (5)	0.4382 (3)	0.043 (2)
C4	0.6265 (6)	0.3862 (4)	0.4377 (3)	0.046 (2)
C5	0.4859 (5)	0.3715 (4)	0.4282 (3)	0.037 (2)
C6	0.4989 (5)	0.0321 (4)	0.3945 (3)	0.035 (2)
C7	0.1446 (4)	0.2940 (4)	0.5075 (3)	0.030 (1)
C8	0.1106 (5)	0.3418 (4)	0.5807 (3)	0.037 (2)
C9	0.1447 (5)	0.2986 (4)	0.6665 (3)	0.041 (2)
C10	0.2130 (4)	0.2092 (4)	0.6833 (3)	0.036 (1)
C11	0.2498 (4)	0.1674 (3)	0.6114 (3)	0.030 (1)
C12	0.0493 (5)	0.4117 (4)	0.3891 (4)	0.041 (2)
C13	−0.0537 (4)	0.1103 (4)	0.3731 (3)	0.039 (2)
C141	0.126 (1)	−0.0087 (7)	0.376 (1)	0.051 (5)
C151	0.0130 (9)	0.0991 (8)	0.2403 (5)	0.034 (3)
C161	0.1303 (9)	0.1119 (6)	0.1987 (6)	0.034 (3)
C171	0.118 (2)	0.294 (1)	0.195 (1)	0.036 (4)
C181	0.3255 (7)	0.2123 (7)	0.2083 (5)	0.028 (3)

cm^{-1}): 1580 (s), 1560 (m), 1550 (s), 1480 (s), 1290 (m), 1260 (s), 1210 (s), 1145 (s), 1070 (m), 1065 (m), 1040 (s), 1000 (m), 950 (m), 780 (m), 760 (s), 730 (s), 700 (s), 625 (m), 435 (m). ($\mu_{eff} = 3.65\ \mu_B$.)

X-ray Crystallography. Complex 1. X-ray data were collected for a crystal (0.10 × 0.22 × 0.63 mm) mounted on a glass fiber and placed under cold nitrogen stream (100 K) of an Enraf-Nonius CAD-4F diffractometer. Crystal data and numerical details on data collection and refinement are given in Table I. Unit cell parameters were derived from least-squares treatment of the SET4 diffractometer angles of 25 reflections in the range $12.4 < \theta < 17.9°$. The monoclinic unit cell was checked for the presence of higher lattice symmetry.[9] Intensity data were corrected for Lorentz and polarization effects and a linear decay of 5.8% during the 50 h of X-ray exposure time. The variance $\sigma^2(I)$ was calculated on the basis of counting statistics plus an instability constant term $(0.064I)^2$ as derived from the excess variance in the reference reflections.[10] The position of vanadium atom was determined by using Patterson methods (SHELXS86).[11] The remaining non-hydrogen atoms were determined from subsequent difference Fourier maps. The electron density of one of the ethylenic TMEDA carbon atoms appeared to be spread out, indicating conformational disorder. A disorder model (54:46) with bond restraints was used in the refinement. Refinement on F was carried out by full-matrix least-squares techniques (SHELX76).[12] Non-hydrogen atoms were refined anisotropically except those affected by disorder, which were refined with isotropic thermal parameters. All the hydrogen atoms were introduced at calculated positions and refined riding on their carrier atom with one common isotropic thermal parameter. Weights were introduced in the final refinement cycles. The maximum residual density was 0.52 e Å^{-3}. Final atomic coordinates and equivalent thermal parameters for the non-hydrogen atoms of the major configuration are listed in Table II. Selected bond distances and angles are given in Table IV. Neutral-atom scattering factors were taken from ref 13 and corrected for anomalous dispersion.[14] All calculations were performed with SHELXS86,[11] SHELX76,[12] and the EUCLID package[15] (PLATON and PLUTON for geometrical calculations and illustrations) on a microVAX cluster.

Table III. Fractional Atomic Coordinates and Equivalent Isotropic Thermal Parameters for **9**

	x	y	z	U_{eq},^{a} Å^2
V1	0.48791 (4)	0.50793 (3)	0.25830 (2)	0.0340 (1)
N1	0.3595 (2)	0.5797 (1)	0.1775 (1)	0.0340 (7)
N2	0.6527 (2)	0.4477 (1)	0.3093 (1)	0.0439 (8)
N3	0.4704 (2)	0.3692 (1)	0.1842 (1)	0.0370 (7)
N4	0.3627 (2)	0.4603 (1)	0.3415 (1)	0.0388 (8)
N5	0.5240 (2)	0.6551 (1)	0.3173 (1)	0.0395 (8)
C1	0.2350 (2)	0.5853 (2)	0.1725 (1)	0.0390 (9)
C2	0.1945 (2)	0.5906 (2)	0.0976 (2)	0.051 (1)
C3	0.2960 (2)	0.5896 (2)	0.0535 (1)	0.053 (1)
C4	0.3942 (2)	0.5840 (2)	0.1035 (1)	0.0383 (9)
C5	0.1614 (2)	0.5925 (2)	0.2404 (2)	0.054 (1)
C6	0.5255 (2)	0.5840 (2)	0.0869 (2)	0.057 (1)
C7	0.7638 (2)	0.4829 (2)	0.2888 (1)	0.052 (1)
C8	0.8552 (2)	0.4317 (2)	0.3275 (2)	0.073 (1)
C9	0.8010 (2)	0.3602 (2)	0.3741 (2)	0.064 (1)
C10	0.6795 (2)	0.3714 (2)	0.3617 (1)	0.048 (1)
C11	0.7758 (2)	0.5614 (2)	0.2278 (2)	0.079 (2)
C12	0.5854 (3)	0.3106 (2)	0.3969 (2)	0.080 (1)
C13	0.3716 (2)	0.3540 (2)	0.1384 (1)	0.042 (1)
C14	0.3591 (2)	0.2719 (2)	0.0884 (2)	0.048 (1)
C15	0.4516 (2)	0.2031 (2)	0.0851 (2)	0.055 (1)
C16	0.5538 (2)	0.2173 (2)	0.1310 (2)	0.055 (1)
C17	0.5606 (2)	0.3007 (2)	0.1792 (2)	0.047 (1)
C18	0.2949 (2)	0.3751 (2)	0.3316 (1)	0.045 (1)
C19	0.2105 (2)	0.3424 (2)	0.3803 (2)	0.052 (1)
C20	0.1916 (2)	0.4003 (2)	0.4440 (1)	0.057 (1)
C21	0.2602 (2)	0.4874 (2)	0.4568 (1)	0.055 (1)
C22	0.3425 (2)	0.5141 (2)	0.4052 (1)	0.047 (1)
C23	0.4631 (2)	0.7404 (2)	0.2970 (2)	0.055 (1)
C24	0.4750 (3)	0.8308 (2)	0.3364 (2)	0.070 (1)
C25	0.5515 (3)	0.8366 (2)	0.3989 (2)	0.068 (1)
C26	0.6142 (2)	0.7503 (2)	0.4212 (2)	0.068 (1)
C27	0.5985 (2)	0.6617 (2)	0.3794 (2)	0.054 (1)

^{a} $U_{eq} = {}^1/_3\sum_i\sum_j U_{ij}a_i a_j \mathbf{a}_i \cdot \mathbf{a}_j$.

Table IV. Selected Bond Distances (Å) and Angles (deg)

1		**9**	
V-N1	2.141 (4)	V-N1	2.169 (2)
V-N2	2.168 (4)	V-N2	2.141 (2)
V-N3	2.158 (4)	V-N3	2.233 (2)
V-N4	2.151 (3)	V-N4	2.152 (2)
V-N5	2.251 (3)	V-N5	2.211 (2)
V-N6	2.242 (4)	N1-V-N2	161.56 (7)
N1-V-N2	62.3 (2)	N3-V-N5	170.72 (7)
N1-V-N3	95.9 (2)	N1-V-N4	98.25 (7)
N1-V-N4	97.1 (1)	N2-V-N4	96.83 (7)
N1-V-N5	93.9 (1)	N3-V-N4	96.83 (7)
N1-V-N6	166.2 (2)	N4-V-N5	92.41 (7)

Complex 9. X-ray diffraction data were collected for a suitable polyfacial crystal sealed in a thin-walled Lindemann glass capillary. Precise lattice parameters and their standard deviations were determined from setting angles of 22 reflections in the range $15.08 < \theta < 16.40°$ in four alternate settings.[16] Reduced cell calculations did not indicate higher lattice symmetry.[17] Space group $P2_1/n$ was determined from systematic extinctions. Three standard reflections were measured every 2 h of X-ray exposure time to monitor crystal deterioration or misalignment, showing consistency throughout the measurements. The intensities of the data were corrected for drift, Lorentz, and polarization effects, but not for absorption. Standard deviations in the intensities based on counting statistics were increased according to an analysis of the excess variance of the three reference reflections.[10] Equivalent reflections were averaged, resulting in 3465 reflections satisfying the $I > 2.5\sigma(I)$ criterion of observability. The structure was solved by using Patterson techniques (SHELXS86)[11] and refined with block-diagonal least-squares techniques (XTAL).[18] All the hydrogen atom positions were located by difference Fourier synthesis. Crystal data and experimental details on crystal structure determination are given in Table I. Fractional atomic coordinates and equivalent isotropic thermal parameters are given in Table III. Molecular geometry data are given in Table IV. Neutral-atom scattering factors[13] were used, with anomalous dispersion corrections,[14]

---

(9) Le Page, Y. *J. Appl. Crystallogr.* **1982**, *15*, 255.

(10) McCandlish, L. E.; Stout, G. H.; Andrews, L. C. *Acta Crystallogr.* **1975**, *A31*, 245.

(11) Sheldrick, G. M. SHELXS86: Program for crystal structure determination. University of Göttingen, FRG, 1986.

(12) Sheldrick, G. M. SHELX76: Program for crystal structure determination. University of Cambridge, England, 1976.

(13) Cromer, D. T.; Mann, J. B. *Acta Crystallogr.* **1968**, *A24*, 321.

(14) Cromer, D. T.; Liberman, D. *J. Chem. Phys.* **1970**, *53*, 1891.

(15) Spek, A. L. The EUCLID package. In *Computational Crystallography*; Sayre, D., Ed.; Clarendon Press: Oxford, England, 1982; p 528.

(16) de Boer, J. L.; Duisenberg, A. J. M. *Acta Crystallogr.* **1984**, *A40*, C410.

(17) Spek, A. L. *J. Appl. Crystallogr.* **1988**, *21*, 578.

(18) Hall, S. R., Stewart, J. M., Eds. XTAL2.2 User's manual. Universities of Western Australia and Maryland.

Scheme I

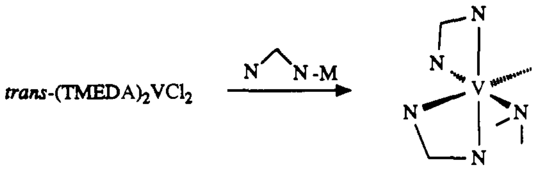

N^N = (2-C_5H_4N)(CH_3)N (1), Ph-N=N-N-Ph (2), 7-azaindolyl (3); Ph-N=C(H)-N-Ph (4), $(C_5H_4N)_2N$ (5); M = Li, Na

Scheme II

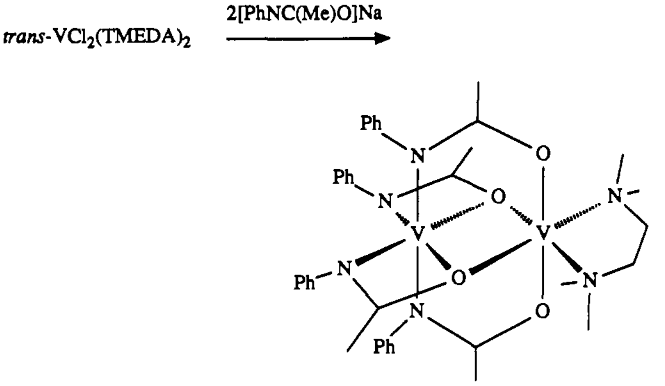

6

for the non-hydrogen atoms. All calculations were carried out on the CDC-Cyber 170/760 computer of the University of Groningen with the program XTAL,[18] the EUCLID package,[15] and an extended version of the program PLUTO (preparation of illustrations).

Results and Discussion

The preparations have been carried out with a standard procedure, by treating *trans*-$(TMEDA)_2VCl_2$ (TMEDA = *N,N,N',N'*-tetramethylethylenediamine)[6d] with 2 equiv of alkali-metal amide (Li, Na). With most of the chelating amides, the reaction led to the formation of monomeric, high-spin, octahedral complexes (Scheme I). A dimeric complex was obtained at room temperature only in the case of the acetanilide ligand, allowing the isolation and characterization of the almost diamagnetic $[PhNC(Me)O]_4V_2(TMEDA)$ dimer (6) (μ_{eff} = 0.42 μ_B) (Scheme II). The structure of 6, as summarized in Scheme II, has been demonstrated by X-ray diffraction analysis.[19] In all the other cases, the dimerization reaction was largely unfavorable, and attempts to enforce dimeric aggregation via thermal dissociation of the residual TMEDA molecule failed. This is probably due to the high stability of the V–N bonds, which indicates, furthermore, that the energy necessary for the dissociation of TMEDA is not compensated by the dimerization reaction.

Considerably different behavior was displayed with monodentate amides. The cyclohexyl derivative Cy_2NLi led to the formation of the homoleptic derivative $[(Cy_2N)_2V]$ (7), probably dimeric (μ_{eff} = 2.28 μ_B), which has been isolated as brown crystals from hexane. In all the other cases (*i*-Pr_2N, Et_2N, $Me_2N(CH_2)_2NMe$), intractable mixtures were obtained, probably due to disproportionation toward V(III) derivatives. The idea that homoleptic V(II) amides may be unstable toward disproportionation is corroborated by the result obtained in the case of Ph_2NNa, which allowed the isolation of a V(II)–V(III) mixed valence species, $[V_3Cl_5(TMEDA)_3][(Ph_2N)_4V]$ (8), through an unusual partial oxidation reaction, which took place during the reaction of *trans*-$(TMEDA)_2VCl_2$ with 2 equiv of Ph_2N-M (M = Li, Na) (Scheme III).[20]

Scheme III

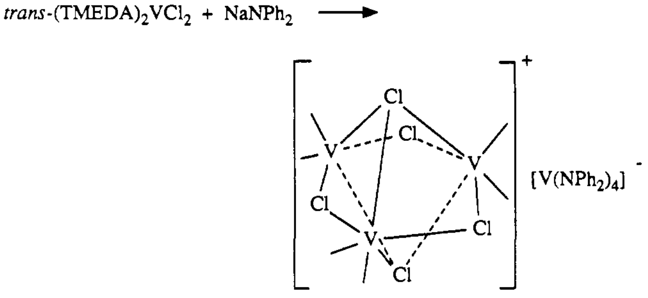

8

Scheme IV

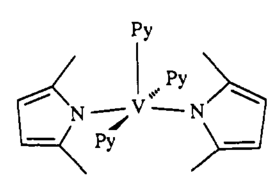

9

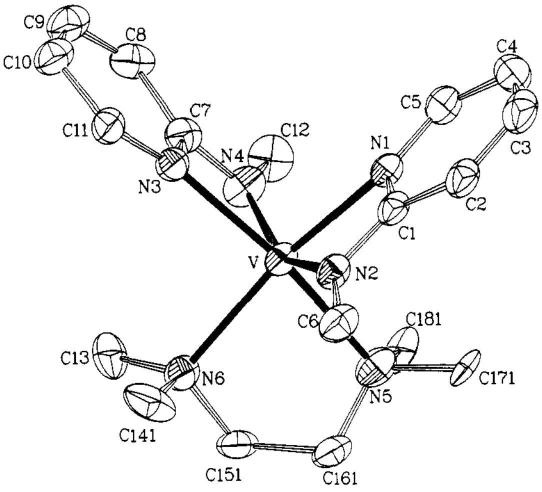

Figure 1. Thermal motion ellipsoid plot (50% probability level) for **1**, with adopted numbering scheme.

In the case of 1, the structure has been determined by X-ray analysis. The structure consists of discrete monomeric units. The distorted octahedral coordination geometry around vanadium is determined by the two chelating aminopyridine ligands, coplanar with vanadium, and the TMEDA molecule, in an overall propeller-shaped configuration (Figure 1). The two inequivalent nitrogen atoms of the aminopyridine fragments have very similar V–N distances [V–N1 = 2.141 (4) Å and V–N2 = 2.168 (4) Å] and are significantly different from those formed by the nitrogen atoms of the TMEDA molecule [V–N5 = 2.251 (3) Å and V–N6 = 2.242 (4) Å]. The angle subtended at the carbon atom by the two aminopyridine nitrogen atoms [N1–C1–N2 = 111.5 (4)°] shows a little contraction from the regular amplitude expected for a sp^2 carbon atom. The geometry of the TMEDA ligand is as expected.

Monomeric, octahedral high-spin species were also formed in the case of the pyrrolyl derivatives (carbazolyl, 3,5-dimethyl-

---

(19) Crystal structure: $C_{38}H_{48}N_6O_4V_2$, M_r = 754.72, triclinic, $P1$, a = 10.293 (1) Å, b = 11.323 (1) Å, c = 17.550 (3) Å, α = 102.01 (2)°, β = 93.02 (2)°, γ = 108.63 (2)°, V = 1880.1 (5) Å^3, Z = 2, R = 0.041 (R_w = 0.046). Edema, J. J. H.; Meetsma, A.; van Bolhuis, F.; Gambarotta, S. *Inorg. Chem.*, in press.

(20) Edema, J. J. H.; Meetsma, A.; Gambarotta, S. *J. Chem. Soc., Chem. Commun.* **1990**, 951.

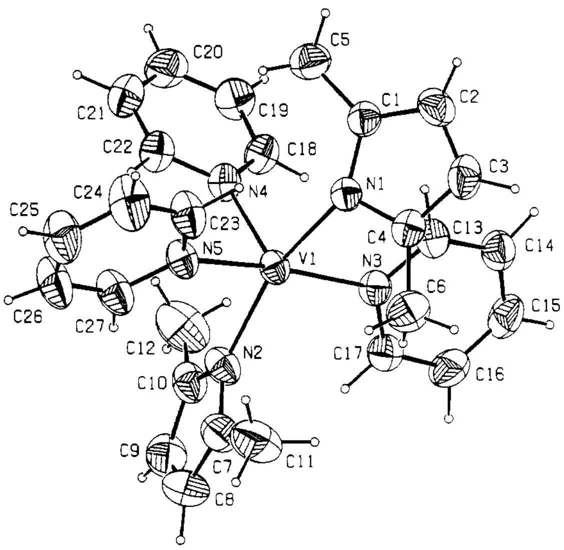

Figure 2. ORTEP plot of **9**. Thermal ellipsoids are drawn at the 50% probability level.

pyrazolyl). An unusual square-based-pyramidal coordination geometry has been observed in the case of the bulky pyrrolyl [2,5-$Me_2(C_4H_2N)$] derivative, which allowed the isolation of monomeric [2,5-$Me_2(C_4H_2N)]_2V(Py)_3$ (**9**) as deep red crystals after treatment with pyridine (Scheme IV).

The overall geometry of the vanadium atom in complex **9**, as demonstrated by X-ray analysis, may be described in terms of a distorted square-based pyramid, with two pyrrolyl groups, two molecules of pyridine, and the vanadium atom defining the basal plane and one additional molecule of pyridine positioned on the apical vertex. In contrast to the case of the isostructural d^4 Cr(II) derivative $(C_4H_4N)_2Cr(Py)_3$,[21] where the axial molecule of pyridine reaches a considerably longer Cr–N distance with respect to the other two basal pyridine molecules, the corresponding distance in complex **9** is slightly shorter [V1–N4 = 2.152 (2) Å versus V1–N3 = 2.233 (2) Å, V1–N5 = 2.211 (2) Å]. The V–N distances of the pyrrolyl groups are as expected [V1–N1 = 2.169 (2) Å, V1–N2 = 2.141 (2) Å] and compare well with those observed in the Cr(II) derivative.[21] The angle subtended at vanadium by the two nitrogen atoms of the two basal pyridine molecules is close to linear [N3–V1–N5 = 170.72 (7)°], while the angle formed by the two pyrrolyl groups is significantly smaller [N1–V1–N2 = 161.56 (7)°], as a probable result of the steric interaction of the two ortho methyl groups with the axial pyridine. In spite of the comparable V–N distances, the two pyrrolyl groups have a curiously different arrangement with respect to the vanadium atom. One ring is in fact coplanar with vanadium, while the second is significantly bent, the distance of vanadium from the ring plane being 0.823 (1) Å. So far, we are unable to explain this feature, since no other particular intramolecular contacts have been found.

The pyramidal geometry of **9** constitutes the first example where this type of geometry is observed in a d^3 system, using a simple monodentate nonmacrocyclic ligand. While a low-spin electronic configuration may be the factor that enforces this unusual coordination geometry in the isostructural Cr(II) (pyrrolyl)$_2$Cr(pyridine)$_3$[21] derivative, this can be excluded in the case of complex **9**, which showed the usual high-spin configuration (μ_{eff} = 3.65 μ_B), commonly observed in octahedral V(II) derivatives.

Acknowledgment. This work was supported by the Natural Sciences and Engineering Research Council of Canada (operating grant) and by the donors of the Petroleum Research Fund, administered by the American Chemical Society. The Nederlandse Organisatie voor Wetenschappelijk Onderzoek (NWO) is gratefully acknowledged for providing a visiting scholarship (J.J.H.E.) and for supporting part of the crystallographic work. X-ray data for **1** were kindly collected by A. J. M. Duisenberg.

Supplementary Material Available: Tables of crystal data, temperature factors, torsion angles, bond angles and distances, thermal parameters, and atomic positional parameters (15 pages); lists of structure factors for **1** and **9** (42 pages). Ordering information is given on any current masthead page.

---

[21] Edema, J. J. H.; Meetsma, A.; van Bolhuis, F.; Spek, A. L.; Smeets, W. J. J. *Inorg. Chem.* **1990**, *29*, 2147.

Contribution from the Department of Chemistry and the Center for Molecular Electronics,
Center for Science and Technology, Syracuse University, Syracuse, New York 13244-4100

Small Heteroborane Cluster Systems. 3. Characterization, Deprotonation, and Transition-Metal Chemistry of the Small Phosphorus-Bridged Pentaborane(9) System (μ-Diphenylphosphino)pentaborane

Bruce H. Goodreau, Robert L. Ostrander, and James T. Spencer*

Received July 26, 1990

The complete spectroscopic characterization of the small phosphorus-bridged pentaborane(9) cluster (μ-diphenylphosphino)pentaborane, [μ-$(C_6H_5)_2PB_5H_8$] (**1**), is reported. The MNDO calculated structure for **1** shows that the B–P–B interaction can be best described as consisting of two two-center–two-electron B–P bonding interactions. Indirect support for the involvement of the lone pair of electrons on the phosphorus in cage bonding is obtained from the failure of **1** to react with [$(CH_3CN)_3Mo(CO)_3$] under forcing conditions. Compound **1** is readily and quantitatively bridge-deprotonated by the action of NaH to produce the corresponding anion, Na[(μ-$(C_6H_5)_2P)B_5H_7$] (**2**). Compound **2** reacts with 1 equiv of [Fe(η^5-C_5H_5)$(CO)_2$I] to yield the iron complex [(μ-$(C_6H_5)_2P)B_5H_7Fe(\eta^5\text{-}C_5H_5)(CO)_2$] (**3**) in high yield as an air-stable, yellow solid. A single-crystal X-ray analysis of **3** shows that the structure consists of a highly distorted square pyramid of boron atoms in which the B(2)–H–B(3) bond in B_5H_9 has been subrogated by a B–P–B bridge and that the [Fe(η^5-C_5H_5)$(CO)_2$] unit is σ-substituted for a terminal proton on B(4). The phosphorus atom exhibits a distorted tetrahedral geometry and is located 0.516 Å below the least-squares basal-B_4 plane. The B(2)–B(3) atomic distance of the B–P–B bridge was found to be 2.68 Å. The structure is formally derived from a two-electron reduction of a *nido*-pentaborane structure by the three-electron-donating phosphino unit to produce an *arachno*-pentaborane structure that is directly analogous to *arachno*-B_5H_{11}. Crystallographic data: space group $P2_1/n$ (No. 14), a = 10.989 (2) Å, b = 13.460 (4) Å, c = 14.454 (5) Å, $\alpha = \gamma$ = 90.00°, β = 95.42 (2), V = 2128 (1) Å^3, Z = 4 molecules/cell.

Introduction

Insights into the synthesis, structure, and bonding of heteroborane polyhedral species provide important information on other classes of substituted main-group and organometallic polyhedra. As part of our continuing interest in the detailed chemistry of phosphorus-containing borane cluster compounds, we are exploring the synthetic and organometallic chemistry of the phosphinopentaborane class of heteroboranes.[1,2] Relatively few small